

Reviewer #1

COMMENT 1: Plot the striation corresponding to the co-seismic slip line deduced from the focal mechanism on the stereoplot of Fig.1

RESPONSE. OK

COMMENT 2: Add orientation of the section on Figure 6

RESPONSE. OK

COMMENT 3: P8 L14, P12 L18, P13 L2 : change whose (for person) into which (for object)

RESPONSE. OK

COMMENT 4: P14 L6-7 : it would be fair to acknowledge, hence to cite here the paper by Lacombe and Mouthereau Tectonics, 2002 entitled : Basement-involved shortening and deep detachment tectonics in forelands of orogens and which therefore fully meets the topic of crustal decollement in deformed forelands.

RESPONSE. OK

COMMENT 5: P15 L10 : SW instead of SE ?

RESPONSE: Yes, it is SW

COMMENT 6: P15-16 : The age of the inherited normal faults is now discussed in more detail than in the previous version, but still fails to explain thickness variation of pre-Permian Paleozoic strata.

RESPONSE. OK. Thickness variation is inferred from a mid-Paleozoic unconformity seen in some seismic sections, including that in figure 5 (below the Miringeh Anticline, at a depth of 2.6-3 seconds). This will be indicated in the new version of figure 5 and it will be mentioned in the text

COMMENT 7: P16 L8 : I would change into 'includes a likely mid-crustal decollement'

RESPONSE. OK

Reviewer#2

COMMENT 1: This is a nice structural reconstruction of the western Zagros, integrating 2017 earthquake data. The main issue is a fixation on the earthquake taking place on a N-S segment of the MFF (Mountain Front Fault). Brief mention is made of the N-S structure being separate – the Khanaqin Fault, but this is then strangely ignored. In fact, it looks very likely that the earthquake took place on the Khanaqin Fault – and is distinct from NW-SE fault segments grouped as the MFF. This is a significant aspect of the regional geology, which should be emphasised rather than underplayed.

RESPONSE. The main-shock and the Khanaqin fault are about 25 km apart. We will show this in figure 3.

COMMENT 2: The root of the problem is that the Zagros faults get depicted in different ways. One view is to emphasise their continuity, so that the MFF, HZF etc get drawn as continuous structures over 100s of km (see Berberian et al 1995). If these faults are offset by N-S right-lateral faults, the offsets are sometimes depicted as up to 100s of km (see Berberian again), but more detailed work shows that such offsets are only a few km (Authemayou et al., 2006). However, the faults are much more segmented than this “Himalayan” style – see work by Walker, Ramsey et al, with segments typically no more than 20-40 km, rupturing in M 5-6 earthquakes. The fault segments linked together as the “MFF” are not a Himalayan-style nappe, but equivalent steps in the relief and geomorphology of the range.

RESPONSE. We did not make this part very clear. We have never supported the idea that the mountain front fault is a continuous structure. Indeed, what we have drawn in figures 1, 2, and 3 is the trace of the mountain front flexure. However, in figures 1 and 2 we have used for the flexure the same pattern as for the faults, and this has created some misunderstanding. Figures 1 and 2 will be modified accordingly.

COMMENT 3: Therefore the Tavani et al paper needs to consider the consequences of the N-S Khanaqin Fault being a separate, N-S structure to the main NW-SE thrusts, which slipped in the 2017 earthquake in a highly unusual manner for the Zagros – witness the sheer size of the event, which is much larger than typical Zagros thrust earthquakes. See Lawa et al (2013) and Allen et al (2013) for examples of Zagros structure maps that include the Khanaqin Fault. The geology descriptions and structural sections look very good, but this issue of fault segmentation and the existence of the Khanaqin Fault means that they need more work.

RESPONSE. We will add the trace of the Khanaqin fault in figure 3. We will also remark that: (1) the Khanaqin fault cannot be the source of the 7.3 earthquake (see point 1), (2) this fault coincides with the backthrust seen at the SW termination of the section (figures 5 and 6).

COMMENT 4: The early part of the paper describes the 2017 earthquake parameters, but another way of doing this is to quote the slip vector azimuth of the event, which is 90 deg. from the auxillary plane strike, ie towards 212 deg. by my calculation. This means highly oblique slip on the fault, and also that the section line in figure 6 is covering faults with very different orientations, from the conventional NW-SE thrusts to the more N-S Khanaqin Fault. Neither of these points comes across properly in the paper.

RESPONSE. The slip vector is more precisely the plane containing the T and P axes, which is also perpendicular to the two nodal planes. This is 215° striking and 78° dipping. As quoted at page 10, the orientation of the section is N49°, i.e. at 14° with respect to the co-seismic slip direction. This direction was chosen because balanced cross-sections must run parallel to the tectonic transport direction, this to ensure the absence of out of plane motion (as quoted in the text). This is a well-established procedure and does not need any further clarification. Concerning the fact that the strike of the nodal plane is oblique to the trend of our section, this is merely because the low-dipping fault is a lateral ramp, and cross-section along lateral ramps must run parallel to the transport direction. Also this basic principle does not need clarification in the text.

Concerning the fact that the section runs oblique to the N-S Khanaqin fault, we remark that if this fault exist, it is a second order accommodation structure, and the section must run perpendicular to the main structures.

COMMENT 5: It would help if the Khanaqin Fault trace was properly drawn on Figures 2 and 3. The authors seem to have taken the continuous, sinusoidal, lines drawn on many regional papers for the Zagros, but, as noted, there are plenty of other papers that try to draw the Khanaqin Fault more accurately.

RESPONSE. Done. Added on figure 3.

COMMENT 6: Where Tavani et al make an improvement on our knowledge is that they try use the 2017 earthquake data to interpret the fault for the first time at depth, as a lateral ramp: this point stands, despite their confusion over the structure being part of the “MFF”. See also Koshnaw et al 2017 for a cross-border geology map that means figure 3 can be improved.

RESPONSE. We will quote Koshnaw et al 2017.

COMMENT 7. A lat/long label in fig 3 should be 45/45 E not 45/45 N.

RESPONSE. Done.

COMMENT 8: Page 3: This structure is thus a candidate...

RESPONSE. Done.

COMMENT 9: The first part of p 15 is critical, as the authors make a good description of the likely regional structure - but this is not apparent on their maps or cross-sections!

RESPONSE. We now explained our view on the N-S striking Khanaqin Fault. If this fault exist, it is the backthrust imaged at the SW edge of the seismic line in figure 5. Accordingly, we have added this at page 13 (Balancing the cross section)

“The position of such a back-thrust roughly coincides with the Khanaqin Fault (e.g. Lawa et al., 2013) (Fig. 3), which accordingly must be downgraded to accommodation structure of the Mountain Front Fault”

In the discussion, at page 16, we have added:

“As previously mentioned, the N-S striking Khanaqin Fault (e.g. Berberian, 1995; Hessami et al., 2001; Lawa et al., 2013; Allen et al., 2013), in our structural reconstruction becomes an accommodation structure of the Mountain Front Fault.”

The back thrust is also labelled Khanaqin Fault in figure 6.

Comments by Ralph Hinsch

COMMENT 1: The balanced section has a local pin in Miringeh Anticline. As a consequence, you end up with some deformation SW of the Mountain Front Flexure (i.e. 4.3km). I haven't seen the deformation front marked on any of the maps as it is further to the SW than the MFF (cf. Verges et al, 2011 Figure 1). Is there really only 4.3 km deformation SW of the MFF?

RESPONSE. The 4.3 km of shortening inferred to the SW of the MFF is highly compatible with published sections across the foreland far to the NW (e.g. Obaid and Allen, 2017). This will be mentioned in the revised version.

COMMENT 2: Then, wouldn't it make sense to extend the section for 5 km, have a fixed pin in the undeformed foreland and show that it restores and balances?

RESPONSE. It would be fine but we have no access to subsurface data to the SE of our pin (Iraq). In addition, only Neogene sediments are exposed there, which is not particularly useful for the construction of deep cross-sections, due to the partial decoupling between Mesozoic and Cenozoic materials.

COMMENT 3: The style how the three inverting faults accommodate shortening seem all different. The style of deformation for the Marakhil and Sheykh Saleh Faults require some coupling with thin skinned decollements to distribute the shortening. The Miringeh Fault inverts straight across these potential decollement zones and then to the SW the suggested fault underneath the MFF links to this decollement at the base of the sediments again.

RESPONSE. The behaviour of the Miringeh fault is well constrained by the seismic section, showing no propagation of any kind of layer-parallel shearing across it. This probably relates with the fact that this fault is in the early stage of inversion, suggesting that coupling mostly occurs due to the development of the footwall shortcut. This will be mentioned

COMMENT 4: A problem with linked thick-thin-skinned contractional systems is that the upper part of a normal fault might be decapitated by the subhorizontal movements on decollement horizons. Could that happen here, if your pin is in the foreland?

RESPONSE. The observation that the major anticlines of the area sit on major basement steps (Sheykh Saleh and Marakhil anticlines), points against the activation of an important decollement level in between the Miringeh and Marakhil anticlines.

COMMENT 5: I find it strange that to the hinterland mainly faults invert and toward the foreland one major shortcut fault exist (the one linked to the MFF). Is that plausible? One solution could be that all major normal faults have been inverted already. Towards SW there are no more major normal faults to invert?

RESPONSE. This is correct, in our interpretation the Miringeh fault is the innermost inherited fault and the MFF is a sort of shortcut of the inherited extensional decollement. This will be made clear.

COMMENT 6: I agree, that the MFF for the Lorestan arc could well be related to basement involvement. But could you discuss alternatives and why they would not work? For other areas along the Zagros the MFF is not necessarily linked to a basement fault (see Hinsch and Bretis, 2015, Geoarabia). For the Kirkuk embayment we propose a duplex solution on multiple arguments. As a consequence we argue that the structure of the MFF is heterogeneous along-strike the Zagros. This might well be in-line with the solution presented here, given the interpreted lateral ramp at the border to the Kirkuk Embayment – but maybe it should be discussed?

RESPONSE. We will mention that the thin-skinned interpretations have been proposed for the MFF. Concerning the discussion about the heterogeneous along-strike significance of the MFF, we think that this is out of the scope of our work.

The seismogenic fault system of the 2017 M_w 7.3 Iran-Iraq earthquake: constraints from surface and subsurface data, cross-section balancing and restoration

Stefano Tavani¹, Mariano Parente¹, Francesco Puzone¹, Amerigo Corradetti¹, Gholamreza
5 Gharabeigli², Mehdi Valinejad², Davoud Morsalnejad², Stefano Mazzoli¹

1 DISTAR. Università degli Studi di Napoli “Federico II”. Napoli, Italy.

2 N.I.O.C., Tehran, Iran.

Corresponding author: Stefano Tavani, stefano.tavani@unina.it

10

Abstract

The 2017 M_w 7.3 Iran-Iraq earthquake occurred in a region where the pattern of major plate convergence is well constrained, but limited information is available on the seismogenic structures. Geological observations, interpretation of seismic reflection profiles, and well data
15 are used in this paper to build a regional balanced cross-section that provides a comprehensive picture of the geometry and dimensional parameters of active faults in the hypocentral area. Our results indicate: (i) coexistence of thin- and thick-skinned thrusting, (ii) reactivation of inherited structures, and (iii) occurrence of weak units promoting heterogeneous deformation within the Paleo-Cenozoic sedimentary cover and partial
20 decoupling from the underlying basement. According to our study, the main shock of the November 2017 seismic sequence is located within the basement, along the low-angle Mountain Front Fault. Aftershocks unzipped the up-dip portion of the same fault. This merges with a detachment level located at the base of the Paleozoic succession, to form a crustal-

scale fault-bend anticline. Size and geometry of the Mountain Front Fault are consistent with a down-dip rupture width of 30 km, which is required for an M_w 7.3 earthquake.

Introduction

5 On November 12, 2017, a M_w 7.3 earthquake struck the north-western portion of the Lurestan region of the Zagros Belt, at the boundary region between Iran and Iraq (Fig. 1). This earthquake had a thrust fault plane solution with a 351° -striking and 16° -dipping nodal plane. The other nodal plane has a strike of 122° and a dip of 79° . The P axis plunges 33° toward 223° , whereas the T axis plunges 54° toward 18° (Fig. 1) (Source: USGS,
10 <https://earthquake.usgs.gov>). These parameters indicate SW-directed co-seismic slip along a low-angle thrust, such a direction being nearly perpendicular to the strike of the Zagros Belt and of its main thrust systems. The hypocenter is located at a depth of ca. 20-km where, according to preliminary teleseismic data, the slip was nearly 9 m (Utkucu, 2017). Coherently with SW-directed motion along a gently dipping thrust, interferometric SAR data show a
15 NW-SE to NNW-SSE-elongated displacement field (Fig. 2). Consistently, the maximum surface deformation (reaching ca. 90 cm of uplift; Kobayashi et al., 2018) is shifted some tens of km SW-ward of the epicentre of the main shock. Forty-five $M_w > 4$ aftershocks followed during the next 30 days in a N-S-elongated, 50x150 km area located to the west of the main shock (Fig. 2). Aftershocks lined up, as most of the major earthquakes of the last 50 years
20 (Berberian, 1995; Talebian and Jackson, 2004), along the Mountain Front Flexure (Figs. 1, 2), a major tectonic lineament of the area. However, the instrumental seismic record indicates that this structure had never produced a $M_w > 7$ earthquake in last decades. Identifying the fault or fault segment activated during the seismic event, and defining its dimensional

parameters, is thus essential for the assessment of the seismic hazard (Wells and Coppersmith, 1994).

In seismically active fold and thrust belts (FTBs), where the earthquake dataset is not sufficiently robust to constrain the geometry of active faults, deep cross-sections built using balancing techniques (Dahlstrom, 1969; Hossack, 1979) have been successfully used to improve the knowledge of the seismogenic structures, as carried out in (e.g.) the Los Angeles area (Shaw and Suppe, 1996; Davis et al., 1989), Taiwan (Yue et al., 2005; Mouthereau and Lacombe, 2006), and the Longmen Shan FTB (Wang et al., 2013). In the Zagros FTB, many of the largest earthquakes are associated with major reverse faults affecting the Precambrian basement (e.g. Jackson, 1980; Berberian, 1995; Talebian and Jackson, 2004), which are included in almost all the published balanced cross-sections across the belt (Blanc et al., 2003; Molinaro et al., 2005; Mouthereau et al., 2007; Vergés et al., 2011). Despite being located more than 200 km away from the epicentral area, these cross sections suggest that the seismogenic structure of the M_w 7.3 earthquake could be related with the Mountain Front Flexure, which extends across the aftershock area of the November 2017 earthquake (Figs. 1,2). The flexure, across which a marked variation of both topography and structural relief occurs (Falcon, 1961), is commonly interpreted as produced by a large underlying basement thrust, namely the Mountain Front Fault. This structure is thus a candidates as the seismogenic fault of the recent M_w 7.3 earthquake.


Geological observations of faults and folds affecting Meso-Cenozoic rocks exposed in the epicentral area are reported in this study. These observations were integrated with the interpretation of near vertical seismic reflection profiles calibrated with well logs, allowing us to produce a detailed and well-constrained geological cross-section reaching a depth ranging from 2 to 5 km. The section was then completed at depth by using the balancing technique

(e.g. Dahlstrom, 1969; Hossack, 1979). Our results indicate that the November 2017 seismic activity is attributable to the Mountain Front Fault, for which, using the balancing technique, we reconstructed 10 km of cumulative displacement in the hypocentral area.

5 Geological background

The NW-SE striking Zagros mountain belt formed due to the continental collision between the Arabian and Eurasian plates (Berberian and King, 1981; Alavi, 1994; 2007; Argand et al., 2005; Mouthereau et al., 2006; Vergés et al., 2011). The present-day northward motion of Arabia relative to fixed Eurasia is about 2 cm/yr (Vernant et al., 2004). This is partitioned between right-lateral motion along NE-SW-striking faults and NE-SW oriented shortening (Blanc et al., 2003; Vernant et al., 2004; Talebian and Jackson, 2002; 2004), which in the Zagros belt is about 5-10 mm/yr (Vernant et al., 2004). The belt is bounded to the NE by the Main Recent Fault and Main Zagros Fault (Fig. 1), forming the suture zone that separates terrains derived from the Mesozoic conjugate margins of the Neo-Tethyan ocean.

10 The Zagros FTB, to the SW of the suture, involves units originally pertaining to the Arabian continental margin (Ziegler, 2001; Blanc et al., 2003; Sepehr and Cosgrove, 2004; Ghasemi and Talbot, 2006; Mouthereau et al., 2012; English et al., 2015). Within the Zagros FTB, the High Zagros Fault, a major structure striking NW-SE, separates the Imbricate Zone to the NE, where intensely faulted and folded units are exposed, from the Folded Belt to the SW

15 (Blanc et al., 2003; Karim et al., 2011; Vergés et al., 2011). The SW boundary of the Zagros FTB is the Mountain Front Flexure, corresponding to a basement and topographic step that divides the belt from its foreland basin to the SW (Falcon, 1961).  flexure is commonly interpreted as being underlined by a thick-skinned basement structure (e.g. Berberian, 1995; Blanc et al., 2003; Vergés et al., 2011), although many researchers have also proposed a thin-

20

[skinned geometry \(McQuarrie., 2004; Hinsch and Bretis, 2015\)](#). The flexure has a sinusoidal shape, defining salients and recesses along the belt. The seismic sequence of the November 2017 earthquake locates at the boundary between two of them, namely the Kirkuk embayment and the Lurestan arc (Figs 1, 2). Folds and thrusts of the Folded Belt of the Kirkuk embayment and of the Lurestan arc are NW-SE-striking, becoming locally NNW-SSE-trending along the boundary between the two domains. There, a major bend of the Mountain Front Flexure occurs (Vergés et al., 2011; Sadeghi and Yassaghi, 2016; [Vashnaw et al., 2017](#)) (Figs. 2,3). Indeed, the envelope of NNW-SSE striking en-echelon folds along the Mountain Front Flexure in the epicentral area of the November 2017 earthquake roughly runs N-S (Fig. 2). This is interpreted as being associated with the occurrence of a N-S-striking basement fault (i.e. the Khanaqin Fault; e.g. Berberian, 1995; Hessami et al., 2001; [Vahdani et al., 2013; Allen et al., 2013](#)) that should presently act as a right-lateral fault. Folds in the Lurestan arc affect an about 10 km-thick sedimentary succession (Hessami et al., 2001; Ziegler, 2001; Homke et al., 2009; Vergés et al., 2011; English et al., 2015). In detail, the uppermost Proterozoic basement of the Arabian plate in the Lurestan region is overlain by a nearly 3000 m thick Paleozoic succession dominated by continental clastic deposits (Jassim and Goff, 2006; Bordenave, 2008). The strong rheological contrast between the crystalline basement and the overlying sedimentary cover makes the basement-cover interface a major decollement horizon of the Lurestan region (e.g. Vergés et al., 2011), despite the lack of evidence for the occurrence of the Hormuz salt at the base of the sedimentary pile of the study area. Permian rifting, related to the opening of the Neo-Tethys ocean (Berberian and King, 1981; Sepehr and Cosgrove, 2004; Ghasemi and Talbot, 2006), led to the deposition of about 1 km of shallow-water carbonates (Chia Zairi Fm.) (Jassim and Goff, 2006; Bordenave, 2008), with at the base some tens of meters of shales, forming a mobile level sandwiched


between two competent packages (Fig. 3). With continuing passive margin subsidence, nearly 1800 m of Triassic-Lower Jurassic shallow-marine carbonates and evaporites, with minor shales, accumulated (Mirga Mir to Sekhaniyan Fm.) (Jassim and Goff, 2006; Bordenave, 2008). This interval is essentially formed by competent units, with the exception of the about 5 100 m thick Baluti and Bedu shales Fms., at the top and base of the Triassic succession, respectively. This is a remarkable difference with respect to the Fars and Dezful Embayment areas to the SE of the Zagros Belt, where the dolostones and limestones of the Triassic Kurra Chine Fm. are substituted by the evaporite-dominated Dashtak Fm., which there acts as a major decollement level. A major late Early to Middle Jurassic subsidence pulse led to 10 carbonate platform drowning and deposition of about 100 m of relatively deep-water limestones, marls and black shales and evaporites (Sargelu, Naokelekan, Barsarin Fm., Toarcian to Tithonian), followed by 700 m of Cretaceous basinal limestones, shales and marls (Garau, Sarvak and Ilam Fms) (Jassim and Goff, 2006; Bordenave, 2008). The closure of the Neo-Tethys Ocean during the Late Cretaceous led to the formation of a flexural basin, filled 15 by a ca. 2 km thick Maastrichtian to Eocene succession (Hessami et al., 2001; Homke et al., 2009; Vergés et al., 2011; Saura et al., 2015), evolving from deep-marine marls and limestones to a prograding wedge of deep marine to continental clastic sediments. This first foredeep infill is overlain by about 500 m of shallow-water carbonates of the Shahbazan and Asmari Fm (Oligocene-lower Miocene), passing upward to lower Miocene evaporites. 20 Renewed shortening and thrusting from the late Miocene to the recent led to the deposition of a younger foreland basin clastic infill (Fig. 3) (Hessami et al., 2001; Jassim and Goff, 2006; Homke et al., 2009).

NE-SW geological cross-section

In this paragraph we present a NW-SE-oriented geological section across the study area. The section is divided into two portions. Figures 4 and 5 illustrate the NE and SW portion of the section, respectively (with a small overlap area). Two seismic reflection profiles running at a low angle to the geological cross-section trace are projected onto the section plane, and key field observations along the NE portion of the section are also reported in figure 4.

The High Zagros Fault to the NE of the study area intersects the cross section of figure 4 in its northern portion. There, the major thrust fault dips roughly parallel to the strata of both hanging-wall and footwall blocks (i.e the cutoff angles are close to zero). Cretaceous strata in the footwall are affected by the NW-SE striking, tens of km-long thrusts of the Satiary Thrust System. These thrusts have low ($< 10^\circ$) hanging-wall and footwall cutoff angles (Fig. 4). Along the section, the Garau Fm. sits in the hanging wall of the thrust and the Ilam Fm. lies in its footwall. However, the geological map of figure 3 shows that the Sehkanian Fm. is the oldest exposed unit in the hanging-wall block and that it is thrust on top of the Upper Cretaceous Gurpi Fm. (see also the field photograph of figure 4), which lies about 1000 m higher in the stratigraphic column. This feature, coupled with the observed hanging-wall flat on footwall flat relationship, suggests displacements in the order of several kilometres. In the footwall of the Satiary thrust system, Upper Triassic to Cretaceous strata are, as a whole, $20\text{-}30^\circ$ NE-dipping for about 4 km, until they meet the tens of kilometres long Herta Thrust System. This includes two 30° -dipping thrusts (joining SE-ward; Fig. 3) showing very low cutoff angles and separating the Triassic Sarki Fm. in the hanging wall of the trailing thrust from the Sargelu and Garau fms. in its footwall (Fig. 4). The repetition of hanging-wall flat on footwall flat geometries (Fig. 4) indicates a remarkable (i.e. several kilometres) displacement also for the Herta Thrust system.

Near-vertical reflection seismic profiles in this northern area are affected by a significant noise; however, both the Satiary and the Herta thrust systems are imaged at depth (Fig. 4) displaying very low cutoff angles, which confirms their significant horizontal displacement. Folds associated with the Herta and Satiary thrust systems are truncated by the High Zagros Fault in the SE portion of the study area. This may be observed in the eastern portion of the geological map of figure 3 and, more in detail, in the photograph of figure 4, where the sub-horizontal High Zagros Fault truncates an anticline exposing the Gurpi Fm. in the limbs and the Ilam Fm. in the core. This observation constrains the relative timing of development of these structures, pointing to an out of sequence emplacement (or reactivation) of the High Zagros Fault, which post-dates the development of the Herta and Satiary fault systems. Moving to the southwest, the Marakhil Anticline exposes the Geli Khana Fm. in its core, and the seismic profile indicates that the Paleozoic strata are folded as well. The Marakhil Fault, bounding the anticline to the SW, has a high ($> 60^\circ$) hanging-wall cutoff angle, typical of a reactivated (i.e. positively inverted) extensional fault (e.g. Sibson, 1985; Williams et al., 1989). The fault flanks to the NE an about 5 km-wide gentle syncline affected by low-displacement (i.e. < 100 m) reverse faults with both low (e.g. the Qlaji Thrust) and high (e.g. the Bawrol Thrust) cutoff angles. In detail, similarly to the Marakhil Fault, the Bawrol Thrust has a hanging-wall cutoff angle typical of a positively inverted normal fault, [whose](#) original extensional activity [of which](#) post-dated the deposition of the Sehkaniyan Fm.. Indeed, syn-kinematic thickening of the Sargelu, Naokelekan, and Barsarin formations (S-N-B in Fig. 4) observed across the Marzan extensional fault, as well as wedging of the same formations in the hanging wall of the Qlaji Thrust, indicate that many of the previously illustrated inverted faults (affecting Triassic and Jurassic strata), developed during a Middle Jurassic extensional pulse. The Sheikh Saleh Anticline is another major structure of this part

of the Lurestan region. It separates an area to the SW, where the oldest rocks exposed in the cores of the anticlines (Gheytureh, Azgaleh, and Miringeh anticlines) belong to the Upper Cretaceous Ilam Fm., from an area to the NE where the oldest rocks exposed at the core of the anticlines belong to the Triassic Kurra Chine and Geli Khana Fms (Fig. 3). The NE block has a structural relief of about 2 km. Despite the significant noise affecting the seismic section, the Ilam and Sehkaniyan Fms. are clearly imaged in the subsurface of the area SE of the Sheikh Saleh Anticline (Fig. 5). Both formations are made of carbonates and are capped by shales and marls of the Sargelu and Gurpi Fms., respectively, this making their top strongly reflective and recognisable. The first clear occurrence of the top Sehkaniyan reflectors is underneath the southwestern limb of the Gheytureh Anticline, at about 1 s TWT (Fig. 5), entirely consistent with the dip and thickness of the overlying stratigraphic units. These Sehkaniyan reflectors are SW-dipping and become NE-dipping about 2 km to the SW, below the syncline flanking to the SW the Gheytureh Anticline. This coherence between surface and subsurface geometries points to a roughly parallel folding of the entire package overlying the Sehkaniyan Fm. About 1 km to the SW, also the top Ilam reflectors become recognisable. Further to the SW, starting from the Azgaleh Anticline area, reflectors are calibrated with well logs and exposures of the top Ilam Fm. In this southwestern portion of the section, the envelope of the top of the Ilam and Sehkaniyan formations defines a 2-5° SW-dipping, regional-scale panel, with limited decoupled deformation between the Mesozoic and Cenozoic units due to the occurrence of a weak package comprised between the stiff Ilam and Asmari Fms. This shallow-dipping faulted and folded panel terminates at the Miringeh Anticline, which displays an unfaulted forelimb. There the strata of the entire Paleozoic to Cenozoic sedimentary succession are parallel and form a 10 km wide SW-dipping monocline.  [In detail, below the Miringeh Anticline, a gentle unconformity occurs between the](#)

Middle and Upper Paleozoic reflectors, evidencing the occurrence of middle Paleozoic deformation- The above mentioned monocline is latter-

is bounded by two N-S striking anticlines cored by the Asmari Fm.; below them, a repetition of the Mesozoic reflectors is observed, which is produced by a backthrust. At the SW termination of the seismic sections, the entire Paleozoic to Cenozoic sedimentary succession becomes horizontal and forms a large-scale syncline.

Balancing the cross-section

The cross-section shown in figures 4 and 5 is completed at depth by producing a geological solution (Fig. 6) in which line-length preservation during folding and thrusting is assumed (e.g. Dahlstrom, 1969; Hossack, 1979). The balanced cross-section is built along a direction oriented N49°, which is perpendicular to the trend of major folds and thrusts. These structures display negligible regional plunge along the section, which allows us to use a vertical plane to build the section. This also ensures the absence of remarkable out-of-plane motion and allows us to directly compute the thickness of the exposed Mesozoic and Cenozoic units along the section. The chosen section plane forms an angle of 17° with the N215°-striking and 78° dipping plane containing the P and T axes of the of the 2017 M_w 7.3 earthquake, thus representing a proper section to obtain insights on the seismogenic structures.

Some lateral thickness variations, in the order of some tens of metres, are observed for the package comprised between the Sargelu and Barsarin fms.. The Sehkaniyan and Sarki fms. also display lateral thickness variations of the same order of magnitude. In the Geli Khana and Kurra Chine fms. we have not observed any kind of growth structure, and the parallelism between reflectors observed in the seismic line of figure 4 indicates that the thickness of these formations can be considered roughly constant. These observations

indicate that, as a whole, a constant thickness can be used for the almost 2 km thick package comprised between the base of the Geli Khana Fm. and the base of the Garau Fm.. The overlying units are not continuously exposed in the northern part of the section and, because of that, they are not shown in the restoration. The Paleozoic units and the basement, for which only limited and discontinuous information is available, are modelled using 1 km and 2 km thick layers, respectively. For the sake of simplicity, thickness variations in Upper Paleozoic units are firstly neglected and then re-introduced after cross-section balancing. This because the adoption of constant thickness for the entire upper crust and of flexural slip folding allowed us to assume line-length preservation. Coherently, the restored cross section shows the cumulative length of Mesozoic, Paleozoic, and basement layers. The trace of the faults in the restored section is obtained by smoothing the polyline built by connecting the restored cutoff points. This is done to avoid zig-zag effects and, in any case, smoothing is less than 0.5% of the original cutoff point position.


Coherently with field observation, in our reconstruction thrusts to the NE of the Marakhil Anticline are thin-skinned and have a displacement in the order of some kilometres. They splay off from a basal decollement located at the bottom of the Triassic sequence, namely within the Bedu Shale, sandwiched between the competent Chia Zairi and Geli Khana-Kurra Chine packages. The Marakhil Anticline is instead a deeply rooted structure, associated with the Marakhil inverted normal fault, which is observed at the surface (Fig. 4). The simple shallow geometry of this large wavelength fold introduces a geometrical problem at depth, as two solutions can be applied to model the deeper portion of the anticline. In the first one, the inverted fault affects only the sedimentary cover, the core of the anticline is filled by ductile material and the underlying basement is not involved in faulting and folding. In the second solution, the inverted fault involves also the basement. The lack of a

sufficiently thick ductile layer at the base of the Paleozoic sequence, and the occurrence of a structural step across the Marakhil Anticline, are more compatible with the second, basement-involved, solution. Following this structural model, and keeping constant the line-length of both basement and cover, we solved the geometry in the core of the anticline by assuming


5 the occurrence of a footwall shortcut of the inverted normal faults in the basement. This represents a typical feature associated with the inversion of normal faults (e.g. McClay, 1989). In our solution, this shortcut transfers displacement from the main reactivated fault to the base of the sedimentary cover. Low-displacement, SW-verging reverse faults and a major back-thrust accommodate such a displacement in the Mesozoic and Paleozoic strata,

10 respectively. The Sheykh Saleh Anticline to the SW shows a similar deep structure, which is even better supported by the remarkable structural step occurring at this location. Here, a positively inverted normal fault with a footwall shortcut occurs in the basement. The footwall shortcut transfers displacement from the main reactivated fault to the base of the sedimentary cover sequence. Such a displacement is accommodated by folding and faulting of the

15 sedimentary cover, with the Paleozoic or Lower Triassic incompetent units (i.e. the Bedu Shale Fm or the shaly level at the base of the Chia Zairi Fm.) promoting decoupling between Mesozoic and Paleozoic strata. In our interpretation, a positively inverted normal fault bounds to the NE the Miringeh Anticline too, producing the uplift of the crustal block in its hanging wall and preventing the southward propagation of the deformation of the

20 sedimentary cover. Indeed, Paleozoic to Cenozoic strata in the crest and in the wide, homogeneously dipping SE limb of this anticline are parallel, unfolded and unfaulted. 

[lack of second-order faults and folds to the SW of the Miringeh inverted fault and their occurrence to the SW of the Marakhil and Sheykh Saleh faults, both the latter faults being characterised by a footwall shortcut, indicates that coupling between the basement and the](#)


sedimentary cover is intimately linked with the shortcut development. Thise SW limb of the Miringeh anticline is underlain by a basement low-angle thrust, corresponding to the Mountain Front Fault, on which the main shock is located (Fig. 6). The focal mechanism provided by the USGS indicates a 351°-striking and 16° dipping thrust fault and, whose its intersection with our N49°-striking vertical section gives 14° of apparent dip. Coherently, in our reconstruction the thrust dips 15° at the hypocentral depth and becomes almost sub-horizontal upward, where it reactivates the basement-cover interface. A back-thrust splays from this upper flat, accommodating part of the displacement transferred from the main ramp of the Mountain Front Fault, and forming together with it a fishtail structure responsible for the surface deformation observed from interferometric data.  position of such a back-thrust roughly coincides with the Khanaqin Fault (e.g. Lawa et al., 2013) (Fig. 3), which accordingly must be downgraded to accommodation structure of the Mountain Front Fault.

An independent quality check of our reconstruction is provided by the top of magnetic basement data (Fig. 6), whose top is computed according to the regional depth map in Teknik and Ghods (2017). The depths of the crystalline basement underlying the sedimentary cover and the top of the magnetic basement obviously do not coincide, due to the heterogeneous nature of the magnetic basement. However, their large-scale shape is similar, confirming the occurrence of highs and lows predicted by our reconstruction. The restored length of the section is 104 km, with a negligible maximum error of 1.5%. The total shortening is 20 km, 8 km of which being associated to the thin-skinned Satiary and Herta thrust systems to the NE of the Marakhil Anticline. As previously mentioned, these thrusts are truncated by the High Zagros Fault, which in this area was active during the Late Cretaceous to Paleocene interval (Karim et al., 2011; Vergés et al., 2011; Saura et al., 2015). These thrusts have also anomalously high displacements compared to the other structures along the

section. For both reasons, the Satiary and Herta thrust systems are interpretable as footwall splay of the High Zagros Fault, probably merging with it to the NE, outside the section. Lower displacements are instead associated with the Marakhil (2.5 km), Sheykh Saleh (2.0), and Miringeh (1.0) faults, the amount of shortening accommodated in the area between the Marakhil and Miringeh anticlines being 5.3 km. The remaining shortening is accommodated by the Mountain Front Fault and associated structures.



Discussion

According to our reconstruction, the Mountain Front Fault has 9.7 km of cumulative displacement at 20 km depth, where the main shock nucleated. The displacement decreases upward, becoming 5.8 km at the upper flat. About 1 km of this is accommodated by the frontal back-thrust, [by the Khanaqin Fault](#), while 4.3 km of shortening is transferred to the foreland structures to the SW of our balanced-cross section. [An expected shortening in the foreland is highly in agreement with data derived from cross-section balancing in the Kirkuk embayment, where 5 km of shortening have been proposed by Obaid and Allen \(2017\).](#) The computed 9.7 km of displacement of the Mountain Front Fault at the hypocentre are broadly consistent with the 13 km proposed for the same structures 200 km to the SE (Blanc et al., 2003; Vergés et al., 2011). The earthquakes of the November 2017 seismic sequence can thus be attributed to movement of the Mountain Front Fault, which forms part of a thrust system splaying from a mid-crustal decollement (Vergés et al., 2011), similar to that documented in other FTBs (Cristallini and Ramos, 2000; [Lacombe and Mouthereau, 2002](#); Butler et al., 2004; Lacombe and Bellahsen, 2016). The important occurrence of reactivated extensional faults documented in this study suggests that the mid-crustal decollement could represent a reactivated inherited extensional decollement (e.g. Marshak et

al., 2000; Tavani., 2012).  [Miringeh fault would be the innermost extensional fault associated with this extensional decollement, and the Mountain Front Fault should be regarded as a sort of crustal shortcut of the reactivated decollement.](#)


Interferometric data show that the maximum surface deformation occurs at the SW
5 edge of the geological section (Fig. 6). This reveals that the coseismic displacement has induced slip along the shallower, near horizontal, upper flat located 20 km to the SW of the main shock, at the basement-cover interface. Decoupling between the Mesozoic and Paleozoic successions, and between Paleozoic strata and the basement, has strong implications in terms of seismic potential. As already pointed out by Nissen et al. (2011),
10 decoupling at the base of the cover sequence implies vertically confined faults, with down-dip width smaller than 8 km. In fact, only four faults affect the entire upper crust: the three major steeply-dipping inverted normal faults splaying out from the basal decollement, probably corresponding to the brittle-ductile transition, and the Mountain Front Fault. The former ones, with their cross-sectional length of up to 25 km, can generate a down-dip
15 rupture width exceeding 8 km, required for an M_w 6 earthquake (Wells and Coppersmith, 1994). On the other hand, the Mountain Front Fault is the only fault on which a down-dip rupture width of 30 km, required for an M_w 7.3 earthquake, may occur.

Beyond their importance for seismic hazard assessments, the data illustrated in this work have major implications in terms of a better understanding of thrust tectonics in the
20 Zagros Mountains. The occurrence of salients and recesses is a common feature in fold and thrust belts (Marshak, 1988) including the Zagros, where different mechanisms are invoked to explain the occurrence of bends in the trace of the Mountain Front Fault ([e.g. Berberian, 1995; Talbot and Alavi, 1996; Bahroudi and Koyi, 2003; Allen and Talebian, 2011; Navabpour et al., 2014; Malekzade et al., 2016, and references therein](#)). According to the

scaling relationship of magnitude vs. rupture area (Wells and Coppersmith, 1994), the rupture area for the Iran-Iraq M_w 7.3 earthquake should exceed 10^3 km². Therefore, the low-angle Mountain Front Fault must extend in the area where the Mountain Front Flexure runs roughly N-S (Figs. 2, 3). This, coupled with the N-S clustering of aftershocks (Fig. 2) triggered by SEW directed co-seismic slip along the low angle thrust ramp, clearly points to the occurrence of a lateral ramp beneath the N-S segment of the Mountain Front Flexure at the boundary between the Kyrkuk embayment and the Lurestan arc.  previously mentioned, the N-S striking Khanaqin Fault (e.g. Berberian, 1995; Hessami et al., 2001; Lawa et al., 2013; Allen et al., 2013), in our structural reconstruction becomes an accommodation structure of the Mountain Front Fault. A further implication of our work concerns the role structural inheritance in the Zagros FTB. The age of rifting and passive margin development is still a matter of debate in the tectonic puzzle of the area. A Permian to Early Triassic age is commonly inferred for the onset of rifting in the Zagros area (e.g. Berberian and King, 1981; Ghasemi and Talbot, 2006). However, we observed extensional structures that developed synchronously with the deposition of the Middle Jurassic Sargelu Fm., the Marzan extensional Fault (Fig. 4) being the most striking one. The positively inverted Marakhil and Bawrol faults, affecting Upper Triassic and Lower Jurassic units (thus younger than the main rifting event) also fit well into an Early to Middle Jurassic extensional episode. Such an extensional pulse could also explain the drowning of the long-lived Triassic-Jurassic carbonate platform and the onset of deep-water conditions in the area (Ziegler, 2001; Jassim and Goff, 2006; Bordenave, 2008). Accordingly, for many of the inverted basement extensional faults, a polyphase extensional history could be proposed, including a Permo-Triassic development and a Middle Jurassic extensional reactivation.  even older, Middle

[Paleozoic origin can be inferred for some of these faults, based on the occurrence of a Middle Paleozoic unconformity seen in some seismic lines \(Fig. 5\).](#)

Conclusions

5 The integration of field data, near vertical seismic reflection profiles, and earthquake data, allowed us to provide a comprehensive picture of the geometry and dimensional parameters of the faults in the hypocentral area of November 2017 seismic sequence at the Iran-Iraq border. The tectonic framework of this area includes a ly mid-crustal decollement level at a depth of ca. 20 km, from which high angle positively inverted normal faults splay off. At its southwestern edge, the decollement ramps up, to form the Mountain Front Fault, which joins southward an upper decollement level located at the basement-cover interface. The occurrence of multiple decollement levels in the sedimentary succession promotes a partly decoupled deformation, and limits the size of most of the faults of the area. The main shock of the November 2017 M_w 7.3 earthquake nucleated in the basement, along the Mountain Front Fault. Co-seismic slip unzipped the shallower portion of the fault to the SW, at the basement-cover interface, and activated structures responsible for the observed surface deformation.

10

15

Acknowledgments

20 We acknowledge the use of imagery from the Land Atmosphere Near-real time Capability for EOS (LANCE) system, operated by the NASA/GSFC Earth Science Data and Information System (ESDIS) with funding provided by NASA/HQ, and of Copernicus Sentinel data 2017, processed by ESA. The geological cross sections presented in this work were constructed using the Midland Valley 3D Move software. Requests for obtaining the near vertical seismic

sections and wells data should be submitted to the National Iranian Oil Company. [We thank two anonymous reviewers and Ralph Hinsch for helping improve an early version of the manuscript.](#)

References

- Agard, P., Omrani, J., Jolivet, L., Mouthereau, F. (2005) Convergence history across Zagros (Iran): Constraints from collisional and earlier deformation. *International Journal of Earth Sciences*, 94, 401-419. DOI: 10.1007/s00531-005-0481-4
- 5 Alavi, M. (1994) Tectonics of Zagros Orogenic Belt of Iran, New Data and Interpretation. *Tectonophysics*, 229, 211-238. DOI:10.1016/0040-1951(94)90030-2.
- Alavi, M. (2004) Regional stratigraphy of the Zagros fold-thrust belt of Iran and its proforeland evolution. *American Journal of Science*, 304, 1-20. DOI: 10.2475/ajs.304.1.1
- 10 Alavi, M. (2007) Structures of the Zagros fold-thrust belt in Iran. *American Journal of Science* 307, 1064-1095. DOI: 10.2475/09.2007.02
- [Allen, M. B., & Talebian, M. \(2011\). Structural variation along the Zagros and the nature of the Dezful Embayment. *Geological Magazine*, 148, 911-924. DOI: 10.1017/S0016756811000318](#)
- 15 [Allen, M. B., Saville, C., Blanc, E. P., Talebian, M., Nissen, E. \(2013\). Orogenic plateau growth: Expansion of the Turkish-Iranian Plateau across the Zagros fold-and-thrust belt. *Tectonics*, 32, 171-190. DOI: 10.1002/tect.20025](#)
- [Bahroudi, A, Koyi, H.A. \(2003\). Effect of spatial distribution of Hormuz salt on deformation style in the Zagros fold and Thrust Belt: An analogue modelling approach. *Journal of the Geological Society*, 160, 719-733](#)
- 20 Berberian, M., 1995. Master “blind” thrust faults hidden under the Zagros folds: Active tectonics and surface morphotectonics. *Tectonophysics*, 241, 193-224. DOI: 10.1016/0040-1951(94)00185-C

- Berberian, M., King, G.C.P. (1981) Towards a paleogeography and tectonic evolution of Iran. Canadian Journal of Earth Sciences, 18, 210-65. DOI: 10.1139/e81-019
- Blanc, E.J.-P., Allen, M.B., Inger, S., Hassani, H. (2003) Structural styles in the Zagros Simple Folded Zone, Iran. Journal of the Geological Society, 160, 401-412. DOI: 10.1144/0016-764902-110
- 5 Bordenave, M.L. (2008) The origin of the Permo-Triassic gas accumulations in the Iranian Zagros Foldbelt and contiguous offshore areas: A review of the palaeozoic petroleum system. Journal of Petroleum Geology, 31, 3-42. DOI: 10.1111/j.1747-5457.2005.tb00087.x
- 10 Butler, R.W.H., Mazzoli, S., Corrado, S., De Donatis, M., Di Bucci, D., Gambini, R., Naso, G., Nicolai, C., Scrocca, D., Shiner, P., Zucconi, V. (2004). Applying thick-skinned tectonic models to the Apennine thrust belt of Italy--Limitations and implications. AAPG Memoir, 82, 647-667.
- Cristallini, E.O., Ramos, V.A. (2000). Thick-skinned and thin-skinned thrusting in the La Ramada fold and thrust belt: crustal evolution of the High Andes of San Juan, Argentina (32 SL). Tectonophysics, 317, 205-235. DOI: 10.1016/S0040-1951(99)00276-0
- 15 Dahlstrom, C.D.A. (1969). Balanced cross sections. Canadian Journal of Earth Sciences, 6, 743-757. DOI: 10.1139/e69-069
- Davis, T.L. Namson, J., Yerkes, R.F. (1989) A cross section of the Los Angeles Area: Seismically active fold and thrust belt, The 1987 Wittier Narrows earthquake, and earthquake hazard. Journal of Geophysical Research: Solid Earth, 94, 9644-9664. DOI: 10.1029/JB094iB07p09644
- 20 English, J.M., Lunn, C.A., Ferreira, L., Yacu, G. (2015) Geologic evolution of the Iraqi Zagros, and its influence on the distribution of hydrocarbons in the Kurdistan region.

American Association of Petroleum Geologists Bulletin, 99, 231-272. DOI:
10.1306/06271413205

Falcon, N.L. (1961) Major earth-flexuring in the Zagros Mountains of south-west Iran.
Quarterly Journal of the Geological Society of London, 117, 367-376. DOI:
5 10.1144/gsjgs.117.1.0367

Ghasemi, A., Talbot, C.J. (2006) A new tectonic scenario for the Sanandaj-Sirjan Zone (Iran).
Journal of Asian Earth Sciences, 26, 683-693. DOI: 10.1016/j.jseas.2005.01.003

Hessami, K., Koyi, H.A., Talbot, C.J., Tabasi, H., Shabanian, E. (2001) Progressive
unconformities within an evolving foreland fold-thrust belt, Zagros Mountains. Journal
10 of the Geological Society, 158, 969-982. DOI: 10.1144/0016-764901-007

[Hinsch, R., Bretis, B. \(2015\). A semi-balanced section in the northwestern Zagros region:
Constraining the structural architecture of the Mountain Front Flexure in the Kirkuk
Embayment, Iraq. Georabia, 20, 41-62.](#)

Homke, S., Vergés, J., Serra-Kiel, J., Bernaola, G., Sharp, I., Garcés, M., Montero-Verdú, I.,
15 Karpuz, R., Goodarzi, M.H. (2009) Late Cretaceous-Paleocene formation of the proto-
Zagros foreland basin, Lorestan Province, SW Iran. Bulletin of the Geological Society
of America, 121, 7-8. DOI: 10.1130/B26035.1

Hossack, J.R. (1979). The use of balanced cross-sections in the calculation of orogenic
contraction: A review. Journal of the Geological Society, 136, 705-711. DOI:
20 10.1144/gsjgs.136.6.0705

Jackson, J.A. (1980) Reactivation of basement faults and crustal shortening in orogenic belts.
Nature, 283, 343-346. DOI: 10.1038/283343a0

Jassim, S. Z., Goff, J. C. (2006) Geology of Iraq: Dolin, Prague and Moravian Museum,
Brno, Czech Republic, 341 pp.

Karim, K.H., Koyi, H., Baziany, M.M., Hessami, K. (2011) Significance of angular unconformities between Cretaceous and Tertiary strata in the northwestern segment of the Zagros fold–thrust belt, Kurdistan. *Geological Magazine*, 148, 925-939. DOI: 10.1017/S0016756811000471

5 | [Lawa, F. A., Koyi, H., Ibrahim, A. \(2013\). Tectono-stratigraphic evolution of the NW segment of the Zagros fold-thrust belt, Kurdistan, NE Iraq. *Journal of Petroleum Geology*, 36, 75-96. DOI: 10.1111/jpg.12543](#)

Kobayashi, T., Morishita, Y., Yarai, H., Fujiwara, S. (2018). InSAR-derived Crustal Deformation and Reverse Fault Motion of the 2017 Iran-Iraq Earthquake in the Northwest of the Zagros Orogenic Belt. *Bulletin of the Geospatial Information Authority of Japan*, in press.

[Koshnaw, R. I., Horton, B. K., Stockli, D. F., Barber, D. E., Tamar-Agha, M. Y., Kendall, J. J. \(2017\). Neogene shortening and exhumation of the Zagros fold-thrust belt and foreland basin in the Kurdistan region of northern Iraq. *Tectonophysics*, 694, 332-355.](#)

15 | [Lacombe, O., Mouthereau, F. \(2002\). Basement-involved shortening and deep detachment tectonics in forelands of orogens: Insights from recent collision belts \(Taiwan, Western Alps, Pyrenees\). *Tectonics*, 21. DOI: 10.1029/2001TC901018](#)

Lacombe, O., Bellahsen, N. (2016). Thick-skinned tectonics and basement-involved fold–thrust belts: insights from selected Cenozoic orogens. *Geological Magazine*, 153, 763-810. DOI:10.1017/S0016756816000078

Malekzade, Z., Bellier, O., Abbassi, M. R., Shabanian, E., Authemayou, C. (2016). The effects of plate margin inhomogeneity on the deformation pattern within west-Central

Zagros Fold-and-Thrust Belt. *Tectonophysics*, 693, 304-326. DOI: 10.1016/j.tecto.2016.01.030

Marshak, S. (1988), Kinematics of orocline and arc formation in thin-skinned orogens, *Tectonics*, 7, 73–86, DOI:10.1029/TC007i001p00073.

5 Marshak, S., Karlstrom, K., Timmons, J.M. (2000) Inversion of Proterozoic extensional faults: An explanation for the pattern of Laramide and Ancestral Rockies intracratonic deformation, United States. *Geology*, 28, 735-738. DOI: 10.1130/0091-7613(2000)28<735:IOPEFA>2.0.CO;2

10 McClay, K. R. (1989). Analogue models of inversion tectonics. Special Publications of the Geological Society of London, 44, 41-59. DOI: 10.1144/GSL.SP.1989.044.01.04

[McQuarrie, N. 2004. Crustal scale geometry of the Zagros fold–thrust belt, Iran. *Journal of Structural Geology*, 26, 519-535.](#)

15 Molinaro, M., Leturmy, P., Guezou, J.C., Frizon de Lamotte, D., Eshraghi, S.A. (2005) The structure and kinematics of the southeastern Zagros fold-thrust belt, Iran: From thin-skinned to thick-skinned tectonics. *Tectonics*, 24, 1-19. DOI: 10.1029/2004TC001633

Mouthereau, F., Lacombe, O. (2006). Inversion of the Paleogene Chinese continental margin and thick-skinned deformation in the Western Foreland of Taiwan. *Journal of Structural Geology*, 28, 1977-1993. DOI:10.1016/j.jsg.2006.08.007

20 Mouthereau, F., Lacombe, O., Meyer, B. (2006). The Zagros folded belt (Fars, Iran): constraints from topography and critical wedge modelling. *Geophysical Journal International*, 165, 336-356. DOI: 10.1111/j.1365-246X.2006.02855.x

Mouthereau, F., Lacombe, O., Vergés, J. (2012) Building the Zagros collisional orogen: Timing, strain distribution and the dynamics of Arabia/Eurasia plate convergence. *Tectonophysics*, 532-535, 27-60. DOI: 10.1016/j.tecto.2012.01.022

Mouthereau, F., Tensi, J., Bellahsen, N., Lacombe, O., De Boisgrollier, T., Kargar, S. (2007). Tertiary sequence of deformation in a thin-skinned/thick-skinned collision belt: The Zagros Folded Belt (Fars, Iran). *Tectonics*, 26, TC5006. DOI: 10.1029/2007TC002098

[Navabpour, P., Barrier, E., McQuillan, H. \(2014\). Oblique oceanic opening and passive margin irregularity, as inherited in the Zagros fold-and-thrust belt. *Terra Nova*, 26, 208-215. DOI: 10.1111/ter.12088](#)

Nissen, E., Tatar, M., Jackson, J.A., Allen, M.B. (2011). New views on earthquake faulting in the Zagros fold-and-thrust belt of Iran. *Geophysical Journal International* 186, 928-944. DOI:10.1111/j.1365-246X.2011.05119.x

[Obaid, A. K., Allen, M. B. \(2017\). Landscape maturity, fold growth sequence and structural style in the Kirkuk Embayment of the Zagros, northern Iraq. *Tectonophysics*, 717, 27-40. DOI: 10.1016/j.tecto.2017.07.006](#)

Sadeghi, S., Yassaghi, A. (2016) Spatial evolution of Zagros collision zone in Kurdistan, NW Iran: constraints on Arabia–Eurasia oblique convergence. *Solid Earth*, 7, 659-672. DOI: 10.5194/se-7-659-2016

Saura, E., Garcia-Castellanos, D., Casciello, E., Parravano, V., Urruela, A., Vergés, J. (2015) Modeling the flexural evolution of the Amiran and Mesopotamian foreland basins of NW Zagros (Iran-Iraq). *Tectonics*, 34, 377-395. DOI: 10.1002/2014TC003660

Sepehr, M., Cosgrove, J.W. (2004) Structural framework of the Zagros Fold-Thrust Belt, Iran. *Marine and Petroleum Geology*, 21, 829-843. DOI: 10.1016/j.marpetgeo.2003.07.006

Shaw, J.H., Suppe, J. (1996) Earthquake hazards of active blind-thrust faults under the central Los Angeles basin, California. *Journal of Geophysical Research*, 101, 8623-8642. DOI: 10.1029/95JB03453

5 | Sibson, R.H. (1985) A note on fault reactivation. *Journal of Structural Geology*, 7, 751-754. DOI: 10.1016/0191-8141(85)90150-6

[Talbot, C.J., Alavi, M. \(1996\). The past of a future syntaxis across the Zagros. *Geological Society of America Special Paper*, 100, 89-109](#)

10 | Talebian, M., Jackson, J. (2002) Offset on the Main Recent Fault of the NW Iran and implications for the late Cenozoic tectonics of the Arabia-Eurasia collision zone. *Geophysical Journal International*, 150, 422-439. DOI: 10.1046/j.1365-246X.2002.01711.x

Talebian, M., Jackson, J.A. (2004) A reappraisal of earthquake focal mechanisms and active shortening in the Zagros mountains of Iran. *Geophysical Journal International* 156, 506-526. DOI: 10.1111/j.1365-246X.2004.02092.x

15 | Tavani, S. (2012). Plate kinematics in the Cantabrian domain of the Pyrenean orogen. *Solid Earth*, 3, 265-292. DOI: 10.5194/se-3-265-2012

Teknik, V., Ghods, A. (2017) Depth of magnetic basement in Iran based on fractal spectral analysis of aeromagnetic data. *Geophysical Journal International*, 209, 1878-1891. DOI: 10.1093/gji/ggx132

20 | Utkucu, M. (2017). Preliminary seismological report on the November 12, 2017 Northern Iran/Western Iraq earthquake. Sakarya University, DOI:10.13140/RG.2.2.17781.27364.

Vergés, J., Saura, E., Casciello, E., Fernández, M., Villaseñor, A., Jiménez-Munt, I., García-Castellanos, D. (2011) Crustal-scale cross-sections across the NW Zagros belt:

implications for the Arabian margin reconstruction. *Geological Magazine*, 148, 739-761. DOI: 10.1017/S0016756811000331

Vernant, P., Nilforoushan, F., Hatzfeld, D., Abbassi, M.R., Vigny, C., Masson, F., Nankali, H., Martinod, J., Ashtiani, A., Bayer, R., Tavakoli, F., Chéry, J. (2004) Present-day crustal deformation and plate kinematics in the Middle East constrained by GPS measurements in Iran and northern Oman. *Geophysical Journal International*, 157, 381-398. DOI:10.1111/gji.2004.157.issue-1.

Wang, M., Jia, D., Shaw, J.H., Hubbard, J., Lin, A., Li, Y., Shen, L. (2013) Active fault-related folding beneath an alluvial terrace in the Southern Longmen Shan range front, Sichuan basin, China: Implications for seismic hazard. *Bulletin of the Seismological Society of America*, 103, 2369-2385. DOI: 10.1785/0120120188

Wells, D.L., Coppersmith, K.J. (1994) New empirical relationships among magnitude, rupture length, rupture width, rupture area, and surface displacement. *Bulletin of the Seismological Society of America*, 84, 974-1002

Williams, G.D., Powell, C.M., Cooper, M.A. (1989) Geometry and kinematics of inversion tectonics. *Special Publications of the Geological Society of London*, 44, 3-15. DOI: 10.1144/GSL.SP.1989.044.01.02

Yue, L.F., Suppe, J., Hung, J.H. (2005) Structural geology of a classic thrust belt earthquake: The 1999 Chi-Chi earthquake Taiwan ($M_w = 7.6$). *Journal of Structural Geology*, 27, 2058-2083. DOI: 10.1016/j.jsg.2005.05.020

Ziegler, A.M. (2001) Late Permian to Holocene paleofacies evolution of the Arabian Plate and its hydrocarbon occurrences. *GeoArabia*, 6, 445-504.